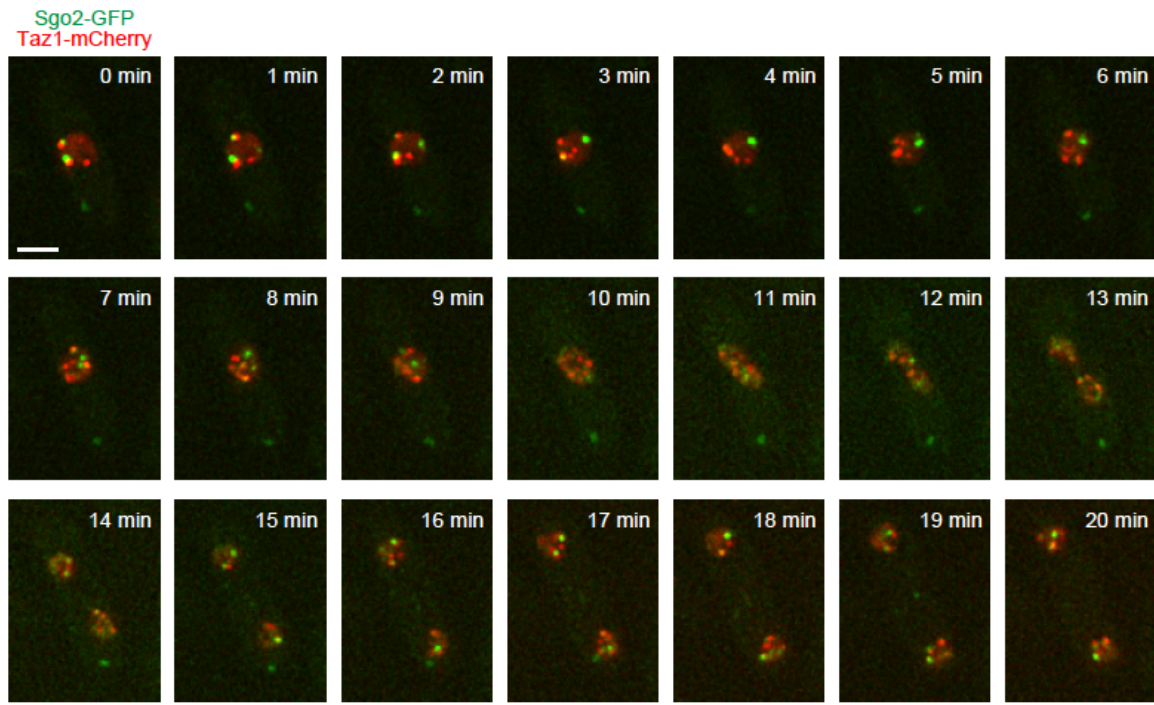


Supplementary Figure 1. Chromosome 3 is devoid of the telomere-proximal subtelomeric common sequences.

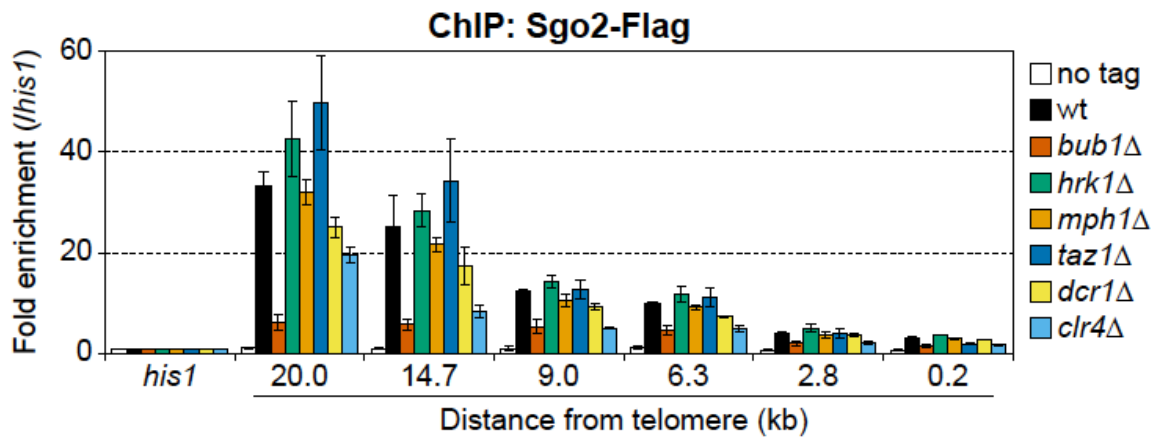
(a) Schematic illustration of the telomere-proximal site of subtelomeres. The restriction map is based on the previously cloned telomere-containing plasmid pNSU70¹.

(b) Pulsed-field gel electrophoresis of the intact three chromosomes of the *S. pombe* wild-type strain, 972 h⁻ followed by Southern blot analysis using TAS (a mixture of TAS1, TAS2, and TAS3)² or rDNA as probes. *S. cerevisiae* chromosomes were used as size markers.



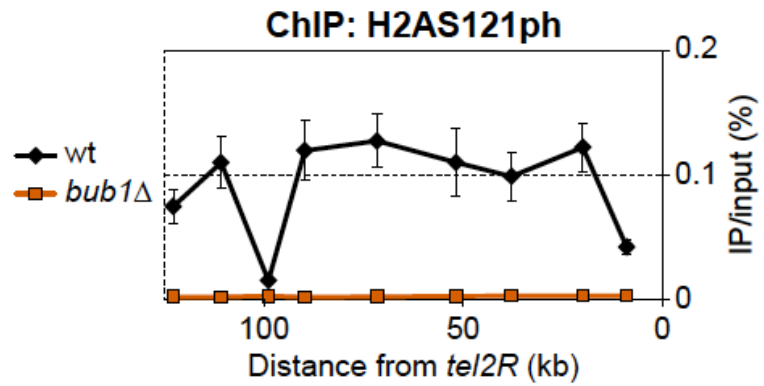
Supplementary Figure 2. Subnuclear localization of Sgo2 in a living cell.

Three-dimensional deconvolved time-lapse images of a single cell grown in EMM at 30°C. Each image is a projection of three-dimensional optical sections. The green signals represent Sgo2-GFP. The red signals represent Taz1-mCherry (telomeres). Sgo2-GFP signals were located near the telomeres at time 0 (the start point of the observation) and began to dissociate from the telomeres at 1 min. Sgo2-GFP was relocated to the vicinity of the telomeres after nuclear division at 13 min. Scale bar, 2 μm.



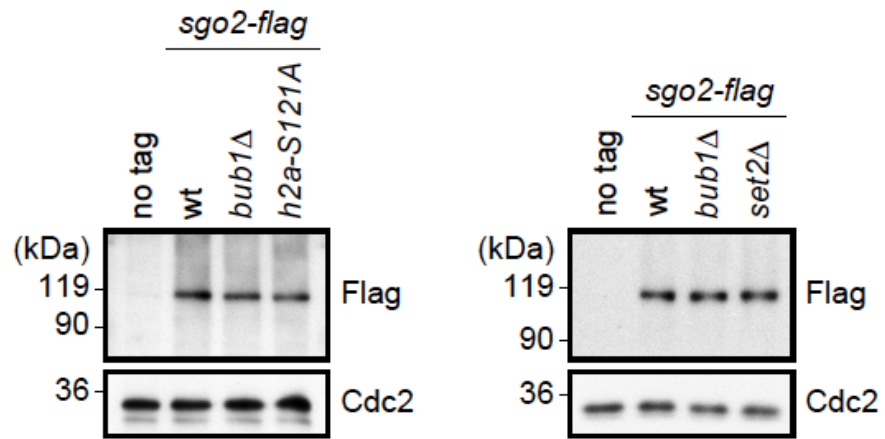
Supplementary Figure 3. Bub1 is important for localization of Sgo2 at the telomere-proximal subtelomeric region.

ChIP analyses of Sgo2-Flag localization at the telomere-proximal subtelomeric region in various mutants. Relative fold enrichment, normalized to the signal at the *his1*⁺ locus, is shown. Error bars indicate the SD ($n = 3$).



Supplementary Figure 4. Lack of H2A-S121 phosphorylation in *bub1Δ* cells.

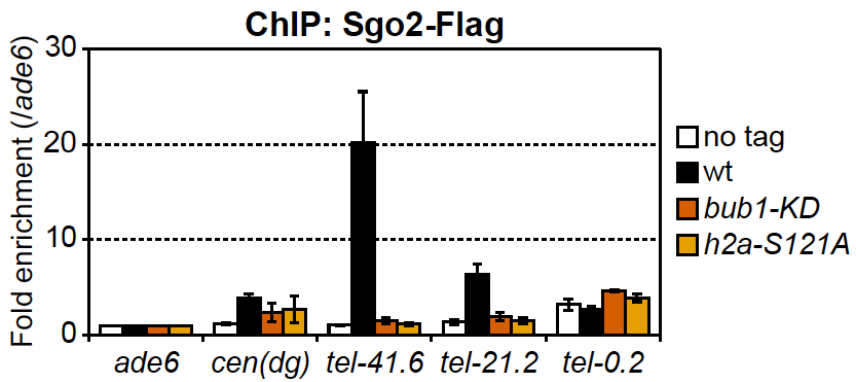
ChIP analyses of phosphorylated H2A-S121 in wild-type and *bub1Δ* cells. The recovery of immunoprecipitated DNA relative to total input DNA was measured by quantitative PCR. Error bars indicate the SD ($n = 3$).



Supplementary Figure 5. Sgo2-Flag protein levels.

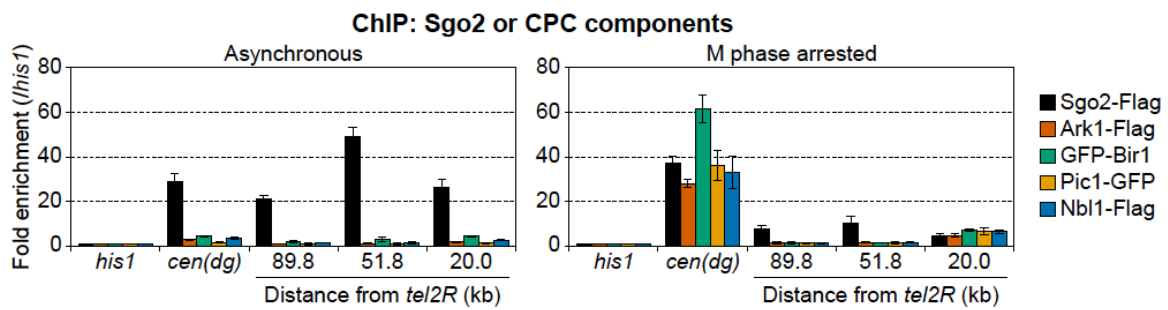
Western blot analysis of Sgo2-Flag protein levels in the strains used in Figs. 3c (left) and 4d (right).

Cdc2 was used as a loading control.



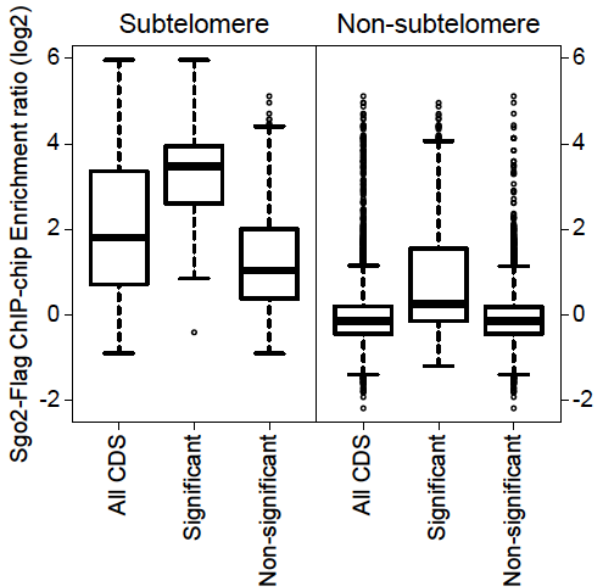
Supplementary Figure 6. Kinase activity of Bub1 is required for the subtelomeric localization of Sgo2.

ChIP analyses of Sgo2-Flag localization in *bub1-KD* (kinase-dead) and *h2a-S121A* mutant cells. Relative fold enrichment at the centromeres (*dg*) and subtelomere loci (*tel-41.6*, *tel-21.2*, and *tel-0.2*), normalized to the signal at the *ade6⁺* locus, is shown. No tag indicates the negative control for the ChIP analysis. Error bars indicate the SD ($n = 3$).



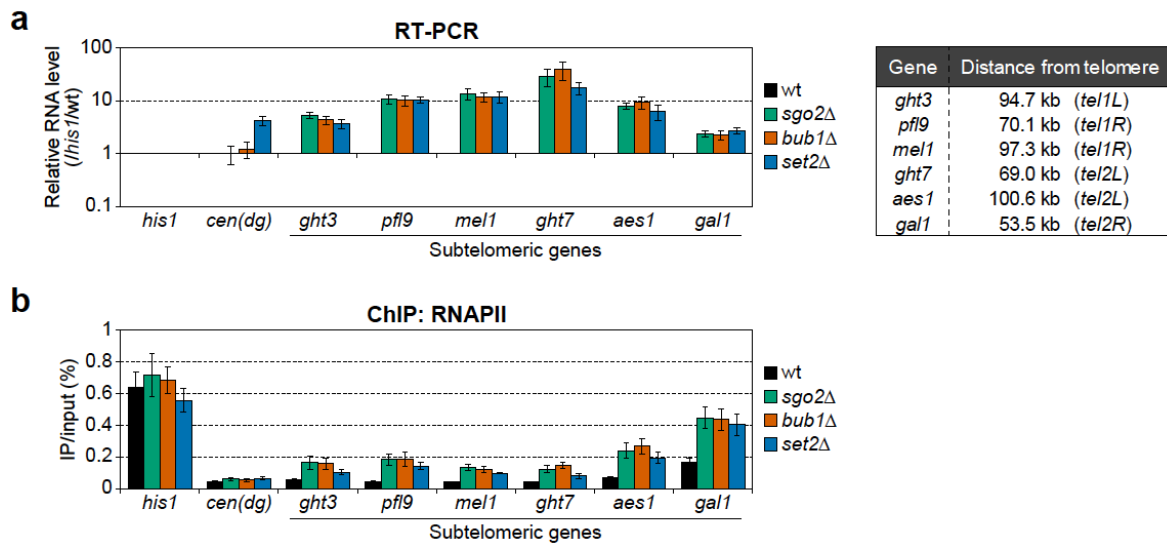
Supplementary Figure 7. CPC components are barely detected at the subtelomeres during interphase.

ChIP analyses of the localization of Sgo2 and CPC components. Cold-sensitive *nda3-KM311* mutant cells were grown at 32°C (asynchronous cells, predominantly in interphase, left) or 20°C for 12 h (M phase-arrested, right) in YPD medium. Relative fold enrichment at *subtel2R*, normalized to the signal at the *his1*⁺ locus, is shown. *cen (dg)* was a positive control for localization of the CPC components. Error bars indicate the SD ($n = 3$).



Supplementary Figure 8. Correlation between Sgo2-dependent gene regulation and the amount of subtelomeric Sgo2.

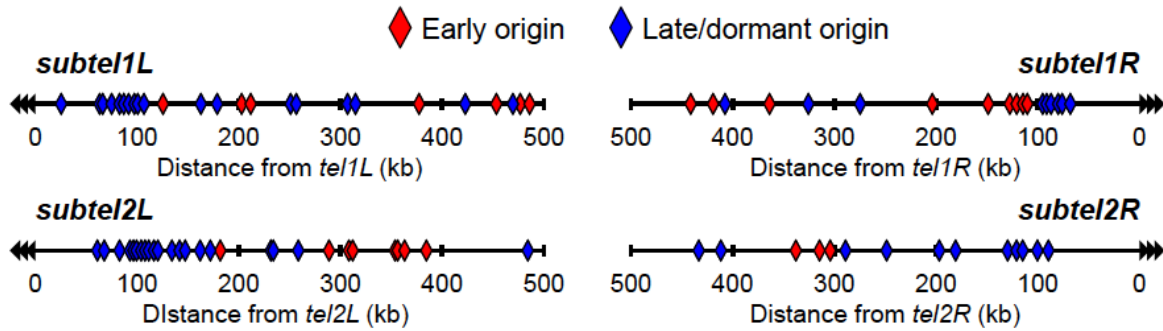
The box plots represent the distribution of the Sgo2-Flag ChIP-chip signals at subtelomeric or non-subtelomeric genes (shown in Fig. 1b), whose expression was significantly affected or not by Sgo2 deletion (shown in Fig. 5a). ChIP-chip array probes that overlapped with the coding DNA sequence (CDS) regions on the expression array were extracted. The box plots summarize the distributions of the ChIP-chip enrichment ratio of the extracted probes. Sgo2 is enriched at the subtelomeric CDS regions, particularly in significant CDS regions, as compared with the non-subtelomeric CDS regions.



Supplementary Figure 9. Set2 is important for gene repression at the subtelomeres.

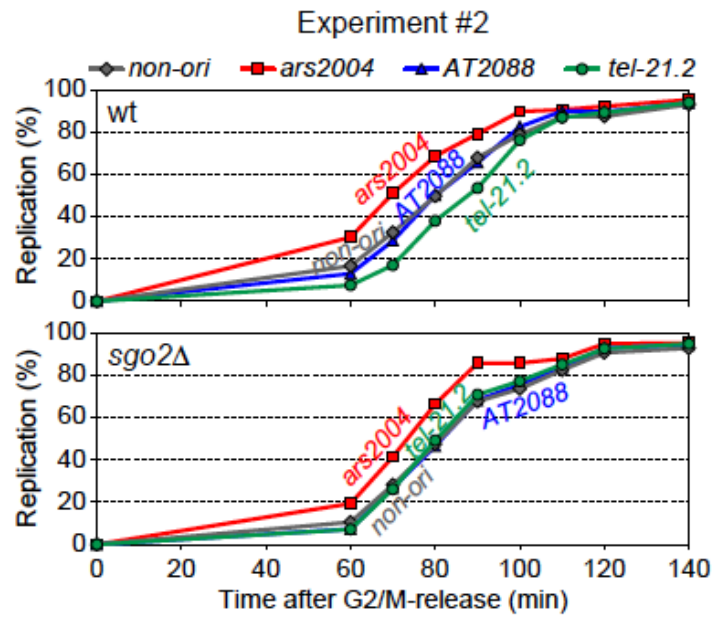
(a) The RNA expression levels of the subtelomeric genes and the centromeric repeats (*dg*) in wild-type, *sgo2Δ*, *bub1Δ*, and *set2Δ* cells were analyzed by quantitative RT-PCR. Each value was normalized to that of *his1⁺*, and then re-normalized to the wild-type value.

(b) The rate of occupancy of RNAPII at the subtelomeric gene loci increased in *sgo2Δ*, *bub1Δ*, and *set2Δ* cells. ChIP analyses of the RNAPII levels at the subtelomeric gene loci and at the centromeric repeats (*dg*). The recovery of immunoprecipitated DNA relative to total input DNA was measured by quantitative PCR. Error bars indicate the SD ($n = 3$).



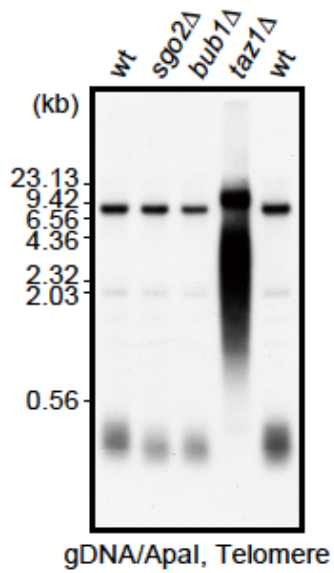
Supplementary Figure 10. Map of the early and late replication origins near the telomeres.

The positions of the early (red) and late (blue) origins near the telomeres identified previously^{3,4} are shown with modification.



Supplementary Figure 11. Independent experimental data confirming the reproducibility of **Figure 7a.**

The experiment was performed as described in Figure 7a.



Supplementary Figure 12. Telomere DNA length in *sgo2 Δ* and *bub1 Δ* cells.

Southern blot analyses of *ApaI*-digested genomic DNA for telomere DNA length. Telomere repeat DNA was used as a probe.

Supplementary Table 1. *S. pombe* strains used in this study

Fig. 1b, c

KM672 $h^- leu1-32 ura4-D18 sgo2-3flag-kan^r$

Fig. 1d

JK107 h^-

ST2915 $h^- sgo2-3flag-kan^r$

Fig. 1e

JP2989 $h^- leu1-32 ura4-D18 taz1-mcherry-hyg^r sgo2-gfp-kan^r gar1-cerulean-nat^r$

Fig. 2a

JK107 h^-

ST2915 $h^- sgo2-3flag-kan^r$

JP776 $h^- leu1 ura4 nda3-KM311 sgo2-3flag-kan^r$

Fig. 2b

ST4229 $h^- leu1-32 ura4-D18 cdc25-22 sgo2-3flag-kan^r$

Fig. 3a

KM1399 $h^{90} ade6-M210 leu1-32 ura4-D18 sgo2-3flag-kan^r$

KM1615 $h^{90} ade6-M210 leu1-32 ura4-D18 trt1::LEU2$ (Type A) $sgo2-3flag-kan^r$

KM1618 $h^{90} ade6-M210 leu1-32 ura4-D18 trt1::LEU2$ (Type B) $sgo2-3flag-kan^r$

Fig. 3b

JK107 h^-

ST2915 $h^- sgo2-3flag-kan^r$

JP3834 $h^- bub1::hyg^r sgo2-3flag-kan^r$

TB3417 $h^- sgo2-3flag-kan^r hrk1::hyg^r$

JP3838 $h^- sgo2-3flag-kan^r mph1::hyg^r$

JP3836 $h^- taz1::kan^r sgo2-3flag-hyg^r$

JP3829 $h^- sgo2-3flag-kan^r dcr1::hyg^r$

JP3844 $h^- clr4::kan^r sgo2-3flag-hyg^r$

Fig. 3c

TB3448 $h^- ade6-M216 leu1-32 sgo2-3flag-hyg^r$

JP3906 $h^- ade6-M216 leu1-32 sgo2-3flag-hyg^r bub1::kan^r$

TB3450 $h^- ade6-M216 leu1-32 hta1(S121A) hta2(S121A) sgo2-3flag-hyg^r$

Fig. 4a

YAM236 $h^{90} sgo2-gfp-hyg^r$

Fig. 4b

YAM055 $h^- taz1-gfp-kan^r$

YAM198 $h^- ade6-216 sgo2::kan^r taz1-gfp-kan^r$

Fig. 4c

972 h^-

PZ876 $h^- ade6-216 leu1 sgo2::kan^r$

AY356-5D $h^- leu1 bub1::kan^r$

YAM081 $h^+ his2 leu1 lys1 ade6-216 set2::kan^r$

JP3415 $h^- ade6-M216 leu1-32$

JP3416 $h^- ade6-M216 leu1-32 hta1(S121A) hta2(S121A)$

Fig. 4d

ST2915 $h^- sgo2-3flag-kan^r$

JP3834 $h^- bub1::hyg^r sgo2-3flag-kan^r$

JP3850 $h^- sgo2-3flag-kan^r set2::hyg^r$

Fig. 5a

JK107 h^-

JP2247 $h^- sgo2::hyg^r$

Fig. 5b

JK107 h^-

JP2247 $h^- sgo2::hyg^r$

KM672 $h^- leu1-32 ura4-D18 sgo2-3flag-kan^r$

Fig. 5c, d, e

JP3415 $h^- ade6-M216 leu1-32$

ST3888 $h^- ade6-M216 leu1-32 sgo2::kan^r$

JP3914 $h^- ade6-M216 leu1-32 bub1::kan^r$

JP3416 $h^- ade6-M216 leu1-32 hta1(S121A) hta2(S121A)$

Fig. 6a

JK107	h^-
JP2247	$h^- sgo2::hyg^r$
JK1330	$h^+ leu1-32 ura4-D18 T2R1-4137:ura4^+$
ST2944	$h^+ leu1-32 ura4-D18 T2R1-4137:ura4^+ sgo2::kan^r$
JK1390	$h^+ leu1-32 ura4-D18 T2R1-4137:ura4^+ swi6::LEU2$
JK1618	$h^- leu1-32 ura4-D18 B2B2-18226:ura4^+$
ST2947	$h^- leu1-32 ura4-D18 B2B2-18226:ura4^+ sgo2::kan^r$
JK1624	$h^- leu1-32 ura4-D18 B2B2-18226:ura4^+ swi6::kan^r$

Fig. 6b

JK1618	$h^- leu1-32 ura4-D18 B2B2-18226:ura4^+$
ST2947	$h^- leu1-32 ura4-D18 B2B2-18226:ura4^+ sgo2::kan^r$
ST3892	$h^- leu1-32 ura4-D18 B2B2-18226:ura4^+ bub1::kan^r$
ST3894	$h^- leu1-32 ura4-D18 B2B2-18226:ura4^+ set2::kan^r$

Fig. 6c

JP2762	$h^- leu1-32 ura4-D18$
JK107	h^-
JP2247	$h^- sgo2::hyg^r$
JK1330	$h^+ leu1-32 ura4-D18 T2R1-4137:ura4^+$
ST2944	$h^+ leu1-32 ura4-D18 T2R1-4137:ura4^+ sgo2::kan^r$
JK1390	$h^+ leu1-32 ura4-D18 T2R1-4137:ura4^+ swi6::LEU2$
JK1618	$h^- leu1-32 ura4-D18 B2B2-18226:ura4^+$
ST2947	$h^- leu1-32 ura4-D18 B2B2-18226:ura4^+ sgo2::kan^r$
JK1624	$h^- leu1-32 ura4-D18 B2B2-18226:ura4^+ swi6::kan^r$
ST3892	$h^- leu1-32 ura4-D18 B2B2-18226:ura4^+ bub1::kan^r$
ST3894	$h^- leu1-32 ura4-D18 B2B2-18226:ura4^+ set2::kan^r$

Fig. 7a, b

HM1864	$h^- cdc25-22 ura4::ura4-Pnmtl-TK ade6::ade6-Padhl-hENT$
HM4771	$h^- cdc25-22 ura4::ura4-Pnmtl-TK ade6::ade6-Padhl-hENT sgo2::hyg^r$

Fig. 7c

HM1864	$h^- cdc25-22 ura4::ura4-Pnmtl-TK ade6::ade6-Padhl-hENT$
HM4771	$h^- cdc25-22 ura4::ura4-Pnmtl-TK ade6::ade6-Padhl-hENT sgo2::hyg^r$
HM5313	$h^- cdc25-22 bub1(K762R,D900N)$

	<i>ura4::ura4-Pnmtl-TK ade6::ade6-Padhl-hENT</i>
HM5259	<i>h- cdc25-22 hta1(S121A) hta2(S121A)</i> <i>ura4::ura4-Pnmtl-TK ade6::ade6-Padhl-hENT</i>
Fig. 7d	
HM2637	<i>h- cdc25-22 nda4-108 ura4::ura4-Pnmtl-TK sld3::sld3-5FLAG-kan^r</i>
HM5280	<i>h- cdc25-22 nda4-108 ura4::ura4-Pnmtl-TK</i> <i>sld3::sld3-5FLAG-kan^r sgo2::hyg^r</i>

Supplementary Fig. 1b

JK107 *h-*

Supplementary Fig. 2

KM994 *h- leu1-32 ura4-D18 taz1-mcherry-hyg^r sgo2-gfp-kan^r*

Supplementary Fig. 3

JK107 *h-*

ST2915 *h- sgo2-3flag-kan^r*

JP3834 *h- bub1::hyg^r sgo2-3flag-kan^r*

TB3417 *h- sgo2-3flag-kan^r hrk1::hyg^r*

JP3838 *h- sgo2-3flag-kan^r mph1::hyg^r*

JP3836 *h- taz1::kan^r sgo2-3flag-hyg^r*

JP3829 *h- sgo2-3flag-kan^r dcr1::hyg^r*

JP3844 *h- clr4::kan^r sgo2-3flag-hyg^r*

Supplementary Fig. 4

JK107 *h-*

JP2251 *h- bub1::hyg^r*

Supplementary Fig. 5

JP3415 *h- ade6-M216 leu1-32*

TB3448 *h- ade6-M216 leu1-32 sgo2-3flag-hyg^r*

JP3906 *h- ade6-M216 leu1-32 sgo2-3flag-hyg^r bub1::kan^r*

TB3450 *h- ade6-M216 leu1-32 hta1(S121A) hta2(S121A) sgo2-3flag-hyg^r*

JK107 *h-*

ST2915 *h- sgo2-3flag-kan^r*

JP3834 *h- bub1::hyg^r sgo2-3flag-kan^r*

JP3850 *h- sgo2-3flag-kan^r set2::hyg^r*

Supplementary Fig. 6

HM4532	<i>h</i> ⁻
HM4846	<i>h</i> ⁻ <i>sgo2-6his3flag-hyg</i> ^r
HM5242	<i>h</i> ⁻ <i>bub1(K762R,D900N)</i> <i>sgo2-6his3flag-hyg</i> ^r
HM5236	<i>h</i> ⁻ <i>hta1(S121A)</i> <i>hta2(S121A)</i> <i>sgo2-6his3flag-hyg</i> ^r

Supplementary Fig. 7

JP776	<i>h</i> ⁻ <i>leu1 ura4 nda3-KM311 sgo2-3flag-kan</i> ^r
JK195	<i>h</i> ⁻ <i>leu1 ura4 nda3-KM311 ark1-3flag-ura4</i> ⁺
KM1378	<i>h</i> ⁻ <i>leu1 ura4 nda3-KM311 gfp-bir1-ura4</i> ⁺
KM1226	<i>h</i> ⁻ <i>leu1 ura4 nda3-KM311 pic1-gfp-kan</i> ^r
TB2635	<i>h</i> ⁻ <i>leu1 ura4 nda3-KM311 nbl1-3flag-kan</i> ^r

Supplementary Fig. 8

KM672	<i>h</i> ⁻ <i>leu1-32 ura4-D18 sgo2-3flag-kan</i> ^r
JK107	<i>h</i> ⁻
JP2247	<i>h</i> ⁻ <i>sgo2::hyg</i> ^r

Supplementary Fig. 9

JK107	<i>h</i> ⁻
JP2247	<i>h</i> ⁻ <i>sgo2::hyg</i> ^r
JP2251	<i>h</i> ⁻ <i>bub1::hyg</i> ^r
JK3846	<i>h</i> ⁻ <i>set2::kan</i> ^r

Supplementary Fig. 11

HM1864	<i>h</i> ⁻ <i>cdc25-22 ura4::ura4-Pnmt1-TK ade6::ade6-Padhl-hENT</i>
HM4771	<i>h</i> ⁻ <i>cdc25-22 ura4::ura4-Pnmt1-TK ade6::ade6-Padhl-hENT sgo2::hyg</i> ^r

Supplementary Fig. 12

JK107	<i>h</i> ⁻
JP2247	<i>h</i> ⁻ <i>sgo2::hyg</i> ^r
JP2251	<i>h</i> ⁻ <i>bub1::hyg</i> ^r
JM2516	<i>h</i> ⁻ <i>taz1::kan</i> ^r

Supplementary Table 2. Primers used to construct the strains

***sgo2* deletion** (PCR-based, other than Fig. 7)

km1	5'-CTTTTGAAACAGAGGAACAGATAG-3'
km2	5'-GGGGATCCGTCGACCTGCAGCGTACGAATAAATAGAAAATCCGATGTACTTC-3'
km3	5'-GTTAACGAGCTCGAATTCATCGATTATGTAATTAAATACCTTCGACATC-3'
km4	5'-AGACATATTATGCCGTTATTAAAC-3'

***sgo2* deletion** (PCR-based, Fig. 7)

HM2863	5'-CCACTGAAAGGATTAGTGAATGG-3'
HM2864	5'-ATCCGTCGACCTGCAGCGTATGTACTTCATTGACCACGTTCC-3'
HM2865	5'-AGATCCACTAGTGGCCTATGCTTCGACATCGTTAGTTGGTTC-3'
HM2866	5'-CTACTTGATGAATGTGCTAAGGTAC-3'

***bub1* deletion** (PCR-based)

jk1021	5'-TTTGCTGCATCCAAGATGATGC-3'
jk1022	5'-GGGGATCCGTCGACCTGCAGCGTACGAGTGATAACGACATTGAAACATGG-3'
jk1023	5'-GTTAACGAGCTCGAATTCATCGATCCTAGAGGGAAAGTTCCATCC-3'
jk1024	5'-GTGCTGACCTCTGGCCTCG-3'

***hrk1* deletion** (PCR-based)

tb75	5'-AGAAACTGTAACCCAGCCCAAGC-3'
tb76	5'-GGGGATCCGTCGACCTGCAGCGTACGAATCTTCCTACATTGTAATATTGAG-3'
tb77	5'-GTTAACGAGCTCGAATTCATCGATTATGGTTTGCACTAAAAAATTG-3'
tb78	5'-CTCAGCGCTATATTCAAGCTTGG-3'

***mph1* deletion** (PCR-based)

jk1671	5'-CTTAGGTGTTTATCCTGAAAG-3'
jk1672	5'-GGGGATCCGTCGACCTGCAGCGTACGAAAACACAGTTACTAAAAACGAGCA-3'
jk1673	5'-GTTAACGAGCTCGAATTCATCGATAGGCACAAATTCCGATTATTCTT-3'
jk1674	5'-TTAGATTTAACTTAGATTTCACAAG-3'

***taz1* deletion** (PCR-based)

jk969	5'-TTGTTTCAGTTGACGTTCTTGTG-3'
jk970	5'-GGGGATCCGTCGACCTGCAGCGTACGATCTGTACTTGCACGCTTATCATC-3'
jk967	5'-GTTAACGAGCTCGAATTCATCGATGTCTCCGGATAGAGTTGTTCATG-3'
jk968	5'-TTGTGCTTCACTCATTACGATTCC-3'

***dcr1* deletion** (PCR-based)

jk639	5'-TAAAATAAAGCATAGGCCTT-3'
jk640	5'-TTAATTAACCGGGATCCGAGGCCGAAGGTTCATTCAATTG-3'
jk641	5'-GTTAAACGAGCTGAATTCTTAAAGTTGACTTGAGACTTG-3'
jk642	5'-AGCAGCTTACGAATCGAAAGAG-3'
<i>clr4</i> deletion (PCR-based)	
jk1467	5'-AGTAATATCCTAACATATGACATATAG-3'
jk1468	5'-GGGGATCCGTCGACCTGCAGCGTACGACGCAAAACTAATAACCTCTGTTG-3'
jk1469	5'-GTTAAACGAGCTGAATTCATCGATCCACTCCTGTTCACCTAATATAGC-3'
jk1470	5'-CTTCACATGTGCGCAGCAGATG-3'
<i>set2</i> deletion (PCR-based)	
jk1675	5'-TTCAAAGATATTGCTACATAAGGC-3'
jk1676	5'-GGGGATCCGTCGACCTGCAGCGTACGATGTATGATAATGGACAAAAGAAAGAG-3'
jk1677	5'-GTTAAACGAGCTGAATTCATCGATTGCCAGTATTTAACTGCGACA-3'
jk1678	5'-TCACCGTTACAGATTATTACTCG-3'
<i>sgo2</i> tagging (PCR-based, other than Supplementary Fig. 6)	
km5	5'-CATCCAATAATTCTCCGTTACG-3'
km6	5'-GGGGATCCGTCGACCTGCAGCGTACGACAAATTAAAGGTTTCGGAGTTTC-3'
km3	5'-GTTAAACGAGCTGAATTCATCGATTATGTAATTAAATACCTTCGACATC-3'
km4	5'-AGACATATTATGCCGTTATTAAAC-3'
<i>sgo2</i> tagging (PCR-based, Supplementary Fig. 6)	
HM3008	5'-AAGGAGCCGAAGGGAACGGAA-3'
HM3009	5'-CCGTGATGATGATGGTGGTCAAATTAAAGGTTTCGGAGTTTC-3'
HM3010	5'-CGCCATCCAGTTAACGAGCCTTCGACATCGTTAGTTGG-3'
HM2866	5'-CTACTTGATGAATGTGCTAAGGTAC-3'
<i>gar1</i> tagging (PCR-based)	
jk1514	5'-ATGGTTGCCAGTCAACCAATG-3'
jk1515	5'-GGGGATCCGTCGACCTGCAGCGTACGAGAATCTGCCACGGAAACCACC-3'
jk1516	5'-GTTAAACGAGCTGAATTCATCGATTGATAAGTATATAAAAGGTTCG-3'
jk1517	5'-TTATTGTGTGGACTGATGACCG-3'
<i>nbl1</i> tagging (PCR-based)	
tb30	5'-AACATCGTCAAGTACGACAGCGAATT-3'
tb31	5'-GGGGATCCGTCGACCTGCAGCGTACGACACTTGCAGTTGAACTCGATT-3'
tb32	5'-GTTAAACGAGCTGAATTCATCGATAACCCTCATCTACTGCTTACTGTG-3'

tb33 5'-AATGGATGGAAATAGGCAAACCTGAAAAC-3'

***taz1* tagging** (Plasmid-based)

jk969 5'-TTGTTTCAGTTGACGTTCTGTTG-3'

jk970 5'-GGGGATCCCGTCGACCTGCAGCGTACGATCTGTACTTGACGCTTATCATC-3'

***ark1* tagging** (Plasmid-based)

jk1173 5'-TATAAAAGATCTCCCTTCGTAAGATAGAAGAGGCC-3'

jk1174 5'-TATAAAGCGGCCGCAGGAAGATTAGAACCTTTGCGAG-3'

***pic1* tagging** (Plasmid-based)

jk1204 5'-TATAAGGTACCACCGCGTCACGTCGAAACCC-3'

jk1205 5'-TATAAAGCGGCCGCATAAAAACCCATGTTTTCTTATAG-3'

Supplementary Table 3. Primer sets used for the quantitative PCR analyses performed in this study

<i>his1</i> (Figs. 1, 2, 3, 4, 5, 6, Supplementary Figs. 3, 7, 9)	
jk1335	5'-CGAAGACGTGCTTCAGCGA-3'
jk1336	5'-TGTCCACCTCGGAATCACTG-3'
<i>cen(dg)</i> (Figs. 1, 2, 3, 5, Supplementary Figs. 7, 9)	
st17	5'-AATTGTGGTGGTGTGGTAATAC-3'
st18	5'-GGGTTCATCGTTCCATTCAAG-3'
<i>cen(dg)</i> (Supplementary Fig. 6)	
	5'- TCCAATGTCGCATGAACACTC-3'
	5'- CTTTTTGGGAATACATTGGGTTT-3'
<i>rDNA</i> (Fig. 1)	
TB19	5'-GGGAACCAGGACTTTACCTTGA-3'
TB20	5'-AACTTGCCTGCTTGAACACTCTA-3'
<i>ura4</i> (Fig. 6)	
st63	5'-GTATTCCAATGTCTGCGAATTG-3'
st64	5'-CATATTGACGTTGTCGAGGATTTC-3'
<i>ade6</i> (Supplementary Fig. 6)	
	5'-TGATGGAGGACGTGAGCACATTGA-3'
	5'-TTGAATGCATCGCAGAGTTGCAGG-3'
<i>subtel2R-0.2 kb</i> (Supplementary Fig. 3)	
jk380	5'-TATTCTTTATTCAACTTACCGCACTTC-3'
jk381	5'-CAGTAGTGCAGTGTATTATGATAATTAAAATGG-3'
<i>subtel2R-2.8 kb</i> (Supplementary Fig. 3)	
jk614	5'-GTCTCGTTGCTCGCTTCACA-3'
jk615	5'-GGAGGATGGGAAATTGAGGAT-3'
<i>subtel2R-6.3 kb</i> (Supplementary Fig. 3)	
jk618	5'-GCCTACCGCTTGCAGTTGTT-3'
jk619	5'-GGTTGAGCATCTGTCAGAGGTAA-3'
<i>subtel2R-9.0 kb</i> (Figs. 2, 3, 3, 4, Supplementary Figs. 3, 4)	
jk620	5'-TTCTTAATCATTATCAAGTATTGCAA-3'
jk621	5'-ACAGTAAACTATGATCGCTTTGAAGAC-3'

subtel2R-14.7 kb (Supplementary Fig. 3)

jk1607 5'-GCTTGGTCAACATCATCTTGTGCG-3'
jk1608 5'-GGGAGCAGCAAGACAAAGGTG-3'

subtel2R-20.0 kb (Figs. 2, 3, 4, Supplementary Figs. 3, 4, 7)

jk455 5'-AACGAGTTGTGCAATGTTAGTAAGGT-3'
jk456 5'-GACCGCTACGCAACCATAAAG-3'

subtel2R-37.9 kb (Figs. 2, 3, 4, Supplementary Fig. 4)

jk690 5'-TGAAACGGGTTCTTACTGCGT-3'
jk691 5'-GCTCCATCCATTGTCATTGGT-3'

subtel2R-51.8 kb (Figs. 1, 2, 3, 4, Supplementary Figs. 4, 7)

jk700 5'-TCCGCAAATTTGTTAGCCAT-3'
jk701 5'-AGCTTAATCGTGATGCAAGTTTTA-3'

subtel2R-71.6 kb (Figs. 2, 3, 4, Supplementary Fig. 4)

km28 5'-CAAAAGCACAAAGGTTGACCA-3'
km29 5'-CCCGACTCCCTAACATGAA-3'

subtel2R-89.8 kb (Figs. 2, 3, 4, Supplementary Figs. 4, 7)

st110 5'-TGC GGACATCATAACATGCTAAA-3'
st111 5'-TTCAATATACACCCGAGGTCCGAAT-3'

subtel2R-98.9 kb (Figs. 2, 3, 3, 4, Supplementary Fig. 4)

km38 5'-TTCAGGATTAAGGTAACGCGGT-3'
km39 5'-TTGCAGTTGTCCGCTAGTGC-3'

subtel2R-110.8 kb (Figs. 2, 3, 4, Supplementary Fig. 4)

km40 5'-CCTATGCCTACGCATTAGCTC-3'
km41 5'-CGATCGTCCACTACTTCACGTTT-3'

subtel2R-122.8 kb (Figs. 2, 3, 4, Supplementary Fig. 4)

st106 5'-AATTTACCGGCTTCGCATCT-3'
st107 5'-TGC GTTTCTCCGTGAATGA-3'

ght3 (subtel1L-94.7 kb) (Fig. 5, Supplementary Fig. 9)

yn120 5'-TTTATCTCAATGTCCGGATGGTT-3'
yn121 5'-CCAAGATGCCGCTAATGGAA-3'

pfl9 (subtel1R-70.1 kb) (Fig. 5, Supplementary Fig. 9)

st49 5'-GCTCTGGCGCCTTGTATTAG-3'
st50 5'-CGCTTCGCTTTGTATCTGTGT-3'

***mell* (subtel1R-97.3 kb)** (Fig. 5, Supplementary Fig. 9)

TB27 5'-TTAGTCGTAAGGATGTGCGTTGTC-3'
TB28 5'-ATCTCCCTGAAGCGCAAAAC-3'

***ght7* (subtel2L-69.0 kb)** (Fig. 5, Supplementary Fig. 9)

st51 5'-AATTGACAGCATCCGGAATTAAG-3'
st52 5'-ATTCCCGCGGTACCGGTATG-3'

***aes1* (subtel2L-100.6 kb)** (Fig. 5, Supplementary Fig. 9)

st37 5'-AAGCTTGCGCCTTAATACATG-3'
st38 5'-CGACAGCTCCTGCACCACTAC-3'

***gal1* (subtel2R-53.5 kb)** (Fig. 5, Supplementary Fig. 9)

jk702 5'-GCGCCTGTTTGTCTCC-3'
jk703 5'-ACGGGCGGTATGGATCAAT-3'

non-ori (Fig. 7, Supplementary Fig. 11)

HM1913 5'-TACGCGACGAACCTTGCATAT-3'
HM1914 5'-TTATCAGACCATGGAGGCCATT-3'

ars2004 (Fig. 7, Supplementary Fig. 11)

HM1911 5'-CGGATCCGTAATCCAACAA-3'
HM1912 5'-TTTGCTTACATTTCGGGAACTTA-3'

AT2080 (Fig. 7)

HM1093 5'-CGAACAAACAGGCTTGGTTAGAA-3'
HM1094 5'-GAAGTACGGACTGTTCGATTCC-3'

AT2088 (Fig. 7, Supplementary Fig. 11)

HM2555 5'-TCCTCACTTCCTAAAAACAGATTAAGAAATA-3'
HM2556 5'-CGCAAAATAACATCGTAGTGGAAC-3'

tel-0.2 (Fig. 7, Supplementary Fig. 6)

HM1627 5'-TATTCTTTATTCAACTTACCGCACTTC-3'
HM1628 5'-CAGTAGTGCAGTGTATTATGATAATTAAAATGG-3'

tel-11.8 (Fig. 7)

HM1635 5'-GCTCTCGACAAAGCCGTTCT-3'
HM1636 5'-CAGCATTAAACCAACAGTGGTCTTC-3'

tel-21.2 (Fig. 7, Supplementary Fig. 6, 11)

HM1132 5'-CAGAAGAGACTACAGAGGCGGTTT-3'
HM1133 5'-GGATGCCTTATCTGCGACCA-3'

tel-30.1 (Fig. 7)

HM3096 5'-AGCAACATGGCAGCACCAT-3'
HM1133 5'-GATAATCGTAAAGCTGGGAATACCA-3'

tel-41.6 (Fig. 7, Supplementary Fig. 6)

HM1639 5'-CGCGCACTTTCGGACATA-3'
HM1640 5'-TGCAAGTCGCCGAAACTACC-3'

tel-45.7 (Fig. 7)

HM1641 5'-TTGAATCCCTCATCCAAAGGA-3'
HM1642 5'-TTGGTGTCAGCCATTGAAC-3'

tel-55.0 (Fig. 7)

HM2103 5'-AAACTGTGACTTCTGCATCGAAT-3'
HM2104 5'-AATCCGGTAATCATAGCTTATAATAAAC-3'

tel-60.0 (Fig. 7)

HM2055 5'-TGCTTCTGTCCATCTAGCTCTGT-3'
HM2056 5'-CGTTGTTGAGATCAGCTACAGTGA-3'

tel-72.3 (Fig. 7)

HM2090 5'-AATTGAGGCATGTAGTGACTCCA-3'
HM2091 5'-CCAGATGGTATCAACAACAAATAATAGA-3'

tel-84.5 (Fig. 7)

HM2086 5'-AGACAATTCAACGGCGAAGA-3'
HM2087 5'-AGTCCTGTCCGGCAGAATCT-3'

tel-94.1 (Fig. 7)

HM2196 5'-GATCTTGGAGGTGCCTATGCTA-3'
HM2197 5'-AAAGGCGAAGAAAATTGTTGAGT-3'

tel-100.8 (Fig. 7)

HM2198 5'-AGAATGAGAGGAGAACGAAGACTTTA-3'
HM2199 5'-CATCGCCTCGTAATTCTGTCTTT-3'

Supplementary References

1. Sugawara, N.F. DNA sequences at the telomeres of the fission yeast *S. pombe*. *Ph.D. Thesis, Harvard University* (1988).
2. Nakamura, T.M., Cooper, J.P. & Cech, T.R. Two modes of survival of fission yeast without telomerase. *Science* **282**, 493-6 (1998).
3. Hayashi, M. et al. Genome-wide localization of pre-RC sites and identification of replication origins in fission yeast. *EMBO J.* **26**, 1327-39 (2007).
4. Tazumi, A. et al. Telomere-binding protein Taz1 controls global replication timing through its localization near late replication origins in fission yeast. *Genes Dev.* **26**, 2050-62 (2012).